Quench development and propagation in metal/MgB$_2$ conductors

E Martínez[1,6]**, F Lera**[1]**, M Martínez-López**[1]**, Y Yang**[2]**,
S I Schlachter**[3]**, P Lezza**[4] **and P Kováč**[5]

[1] Instituto de Ciencia de Materiales de Aragón, CSIC - Universidad de Zaragoza, C/ María de
Luna 3, 50018 Zaragoza, Spain

[2] Institute of Cryogenics, School of Engineering Sciences, University of Southampton,
Southampton SO17 1BJ, UK

[3] Forschungszentrum Karlsruhe GmbH, Institut für Technische Physik, PO Box 3640,
76021 Karlsruhe, Germany

[4] Group of Applied Physics, University of Geneva, 20, rue de l'Ecole de Medecine CH-1221
Geneva 4, Switzerland

[5] Institute of Electrical Engineering, Slovak Academy of Sciences, Dúbravska cesta 9,
841 04 Bratislava, Slovakia

Abstract
The thermal stability of different Fe- and Ni-sheathed MgB$_2$ conductors has
been studied experimentally and numerically, focusing on the estimation of
the quench propagation velocities, v_p, minimum quench energies (MQEs)
and minimum propagating zones (MPZs). The measurements have been
done at self-field and under adiabatic conditions, at variable temperatures
and transport currents. Energy pulses were deposited to the conductor by
passing rectangular current pulses through a graphite-based epoxy heater.
The measured voltage around the heater together with numerical simulation
allows the estimation of the minimum propagating zone. Moreover, v_p was
obtained by measuring multiple voltage taps and thermocouples attached
along the conductor. The effect of the current sharing temperatures, $I_c(T)$,
of the superconductor, and thermal and electrical properties of the metal
sheath have been analysed. The experimental results are in qualitative
agreement with the simulated ones, obtained by solving the one-dimensional
heat balance equation of the system.

(Some figures in this article are in colour only in the electronic version)

1. Introduction

The analysis of the thermal stability behaviour of metal/
superconductor composites is essential for their use in electric
power applications, since the occurrence of disturbances
during normal operation may cause the transition from
superconducting to normal state of the entire wire, so-called
quench. MgB$_2$ superconductor has been revealed as a suitable
candidate for practical large-scale applications at operation
temperatures in the range 20–30 K, easily reachable with
cryocoolers. Nowadays, special efforts are being made to
develop long metal/MgB$_2$ wires and tapes with enhanced
superconducting and magneto-thermal stability properties.

[6] Author to whom any correspondence should be addressed.

The powder-in-tube (PIT) method constitutes one of the most
attractive technologies for long-wire fabrication of hard and
brittle materials due to its potential scalability and production
flexibility.

Two basic routes using Mg + B powder mixtures (*in situ*)
or MgB$_2$ powder (*ex situ*) deformed in a metallic sheath
are mostly used for composite MgB$_2$ wires [1–4]. The *ex
situ* process needs relatively high temperature ($\approx$950 °C) for
the final heat treatment to allow the complete MgB$_2$ core
recrystallization [2, 4]. The annealing for the *in situ* route can
be done at much lower temperatures (640–750 °C) [4–6]. Pure
iron was considered as one of the best sheath materials from
the point of view of formability and chemical compatibility
with MgB$_2$ [2], though a reaction between the MgB$_2$ core

Table 1. Parameters of the analysed metal/MgB$_2$ conductors. K and R are the thermal conductivity and the resistance of the composite, respectively. Thermal properties of these samples are in reference [23].

Sample ID	Sheath	Description	Transversal dimensions	f_{sc}	K (W K^{-1} m^{-1}) at 40 (K)	R (300 K)/R (40 K)
Fe4SW	Fe	4-filament square wire, *ex situ* [19]	1×1 mm^2	0.25	20	4.9
FeRW	Fe	1-filament round wire, *in situ*	$\phi = 1.18$ mm	0.30	39	6.1
FeT	Fe	1-filament tape, *ex situ* [21, 22]	4.1×0.42 mm^2	0.35	12	2.7
NiRW	Ni	1-filament round wire, *ex situ* [20]	$\phi = 1.20$ mm	0.35	59	11.7

and iron sheath has been observed [4]. The reactive interface layer (mostly iron borides, FeB, Fe$_2$B) is very hard and highly resistive, influencing the transfer of current [7] and also heat, which considerably decreases the thermal stability of Fe-sheathed conductors.

The improvement of thermal stability of these conductors should be reflected in the increase of the value of the parameters describing the quench development, such as quench propagation velocity, v_p; minimum quench energy, MQE, which is the energy necessary to trigger a quench; and the minimum propagating zone, MPZ, or minimum zone that should transit to normal state in order to develop a quench.

Although thermal stability has been widely studied for low-temperature superconductors (LTSs) [8–11], and for high-temperature superconductors (HTSs) [12–14], there are just a few experimental [15] and numerical results [16] on quench propagation of MgB$_2$ composite conductors. It is known that quench development and evolution differs in HTS and LTS conductors, mainly due to the different operation temperatures, critical temperatures, n-values of their I–V curves and temperature interval over which the device remains superconducting. These are mainly reflected in different quench processes (generally, normal-zone propagation in LTSs and thermal runaway in HTSs) as well as in different v_p and MQE values [17, 18].

In this paper we present the experimental and calculated results of normal-zone development and propagation for point disturbance measurements, focusing on the analysis of v_p, MQE, and MPZ, for MgB$_2$ composite conductors of different metal sheaths fabricated by the PIT technique. The measurements were done at self-field and under adiabatic conditions on 10 cm long samples, at variable operation temperatures, 15 K $\leqslant T_0 \leqslant$ 30 K, and transport currents, 40 A $\leqslant I \leqslant$ 120 A. The numerical results have been obtained by solving the one-dimensional (1D) heat balance equation of the system. The comparison between the results obtained numerically and experimentally is presented. Moreover, the numerical simulation has allowed us to determine that the conductor length used here is sufficient for quench propagation experiments, and therefore that the observed behaviour is applicable to longer samples for the analysed conductors at the different current and temperature conditions.

2. Experimental details

The conductors used in this study have been prepared by the conventional PIT method using the *in situ* and *ex situ* reaction techniques and Fe and Ni as sheath materials. The main parameters describing the conductors are collected in table 1. For the FeRW conductor a powder mixture with Mg:B ratio
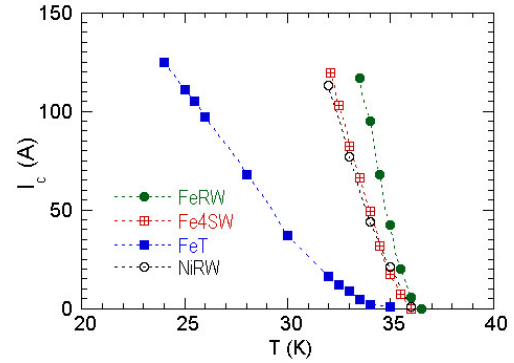
Figure 1. Temperature dependence of the critical current of the studied samples in self-field.

of 0.9:2 was filled in an Fe tube (purity 99.5%) with 10 mm outer diameter and 1.5 mm wall-thickness in an Ar atmosphere. The wire was then swaged to 4.9 mm diameter, heat-treated at 595 °C for 1 h (heating ramp 200 °C h^{-1}, furnace cooling) to release stresses in the Fe sheath and then swaged to 1.2 mm diameter. The final heat treatment was performed for 1 h at 625 °C (heating ramp 200 °C h^{-1}, furnace cooling). The fabrication procedure of the other measured wires and tapes is described in detail elsewhere [19–22].

The $I_c(T)$ of the samples at self-field, measured using triangular current pulses (duration 1 s), is shown in figure 1. The obtained n-values of the I–V curves are high for all samples, and increase sharply with temperature, typically from $n = 10$ at 35.7 K up to $n > 50$ for $T > 34$ K. The FeT tape shows the sharpest transitions and in most cases the n-value cannot be measured, as it quenches during measurements, and therefore their I_c-values may be underestimated.

Figure 2 shows a schematic diagram of the heater, voltage taps and thermocouple locations used in the measurements. In the experiments, the energy was deposited to the wire (carrying a current, $I < I_c$) by passing a rectangular current pulse of variable duration (typically $t_p = 5$–50 ms) to a heater made of a graphite based paste (ECCOBOND 60L) [9]. The length of the heater, L_h, is about 2–3 mm, and its resistance may vary between 0.5 and 5 Ω. A thin layer of silver paint between the sheath and the eccobond was used in order to get reproducible resistances in this range. In order to minimize the thermal contact resistance between the heater and the sample, the superconductor is used as the return path of the heater current, I_h. The energy pulse deposited on the conductor is $Q_{ini} = V_h I_h t_p$, where I_h is obtained by using a calibrated resistance in series with the heater, and V_h is measured by the standard four-point procedure (figure 2). For quench propagation experiments, these heaters are preferable to the
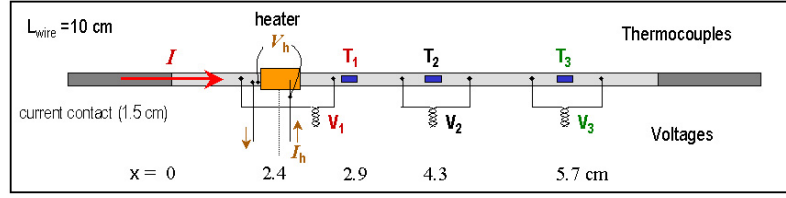
Figure 2. Schematic diagram of the heater, voltage taps and thermocouple positions for quench propagation experiments. The length of the voltage taps is $L_1 = 1.0$–1.2 cm for V_1 and L_2 and $L_3 = 0.5$–0.6 cm for V_2 and V_3.

resistive heaters that are insulated from the wire, since the thermal time constant of the heater–wire system is usually large and not well controlled.

Each sample was mounted in a cryocooled cryostat and was thermally anchored to the second stage of the cold head of the cryocooler. The measurements were done in vacuum and at different temperatures, from 15 to 40 K, using a Lakeshore 331 temperature controller. The temperature profile along the conductor was measured by K-type thermocouples, which were soldered to the sample in order to minimize the thermal contact resistance, and using the cold finger as the reference temperature. The voltage development and temperature along the conductor were monitored by a data acquisition (DAQ) device. In order to prevent the damage of the conductor after a quench, the current is turned to zero at 0.3–2.0 s (depending on the current and the sample) after injecting the energy pulse.

3. Numerical simulation

Assuming uniform temperature over any cross section of the conductors, the time evolution of the temperature along the wire has been obtained by solving the one-dimensional (1D) heat flow equation [10]:

$$\frac{\mathrm{d}}{\mathrm{d}x}\left(K\left(T\right)\frac{\mathrm{d}T}{\mathrm{d}x}\right) + \frac{IE(T)}{A} + q_{\mathrm{ini}}\left(x,t\right) - C(T)\frac{\mathrm{d}T}{\mathrm{d}t} = 0 \quad (1)$$

where x is the distance along the wire, t time, T temperature, A area of the cross section, $K(T)$ and $C(T)$ are the thermal conductivity and the specific heat per unit volume of the conductor, respectively, q_{ini} (W m^{-3}) $= Q_{\mathrm{ini}}/(L_{\mathrm{h}}A)$ is the initiating energy pulse, I is the transport current flowing through the wire and E is the electric field along the wire, which depends on the temperature. The resulting joule heating per unit volume, $IE(T)/A$, has been calculated by assuming the metal matrix and the superconductor as two impedances connected in parallel:

$$E(T) = \begin{cases} \rho_{\mathrm{m}}(T)J_{\mathrm{m}}(T), & \text{in the matrix} \\ E_0\left[\dfrac{J_{\mathrm{sc}}(T)}{J_{\mathrm{c}}(T)}\right]^n & \text{in the supercond.} \end{cases} \quad T < T_{\mathrm{c}}$$

$$E(T) = \rho_{\mathrm{n}}(T)\frac{I}{A} \qquad T > T_{\mathrm{c}} \tag{2}$$

with

$$I = I_{\mathrm{m}} + I_{\mathrm{sc}} = (1 - f_{\mathrm{sc}})AJ_{\mathrm{m}}(T) + f_{\mathrm{sc}}AJ_{\mathrm{sc}}(T), \quad (3)$$

f_{sc} being the superconductor fractional area, ρ_n the resistivity of the composite in the normal state, ρ_{m} the resistivity
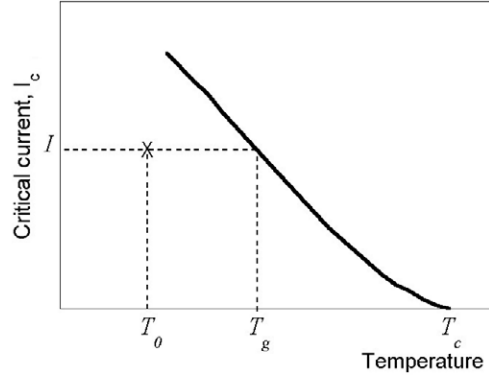

Figure 3. Schematic diagram of the critical current as a function of temperature showing the current sharing temperature, T_{g}, and the initial conditions (marked by an 'X') of quench propagation experiments.

of the metal matrix and $E_0 = 10^{-4}$ V m^{-1}. As a first approximation we have considered here that the normal resistance of the composite is dominated by the resistance of the sheath. In equation (2), J_{c} is the critical current density of the superconductor ($J_{\mathrm{c}} = I_{\mathrm{c}}/f_{\mathrm{sc}}A$), which depends on the temperature (figure 1). The current share of the superconductor and the metal matrix, I_{sc} and I_{m}, respectively, should satisfy equation (3) for a given transport current I, and can be expressed in the corresponding current density values J_{sc} and J_{m}. Equation (1) has been solved numerically with the contour conditions $T(x = 0) = T(x = L) = T_0$, using the thermal and electrical properties measured on conductors from the same batch [23] and the experimentally obtained $I_{\mathrm{c}}(T)$ curve. From the calculated $T(x, t)$ and $E(x, t)$, the voltages V_1, V_2 and V_3, are obtained in order to compare them with the experimental measurements.

In both experiment and calculation, the sample is initially (at $t = 0$) at a uniform temperature T_0 below T_{c} and carries a given current I well below the corresponding critical current $I_{\mathrm{c}}(T_0)$, so that there is not heat generating in the wire (see figure 3). After applying Q_{ini}, the temperature increases, and when approaching the critical current curve, the wire dissipates energy. For high n-values it is normally considered that the dissipation starts at T_{g}, the so-called current sharing temperature [8]. As indicated in figure 3, T_{g} depends on the applied current, $T_{\mathrm{g}}(I)$ being the inverse function of $I_{\mathrm{c}}(T)$.

4. Results and discussion

For all the analysed samples, it is seen that when the applied Q_{ini} is higher than a certain value, a normal zone is created
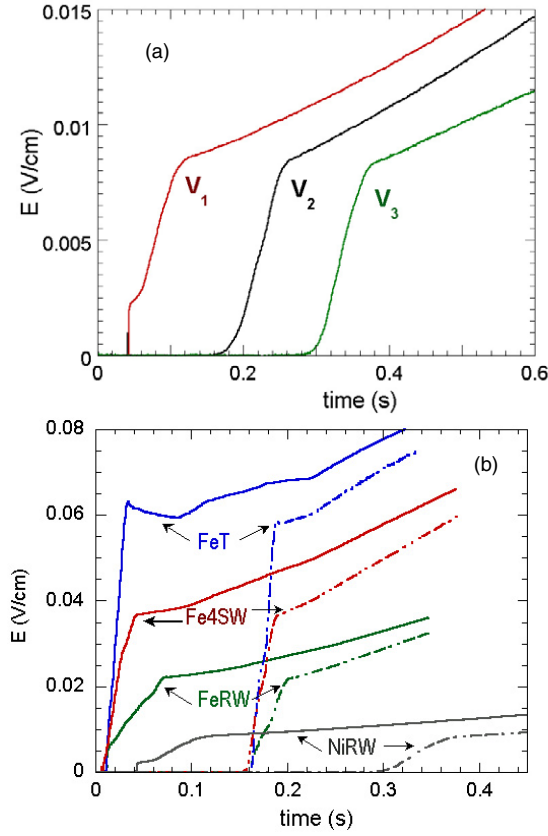
145

Figure 4. Measured voltages at $T_0 = 20$ K and $I = 100$ A during a quench (a) along the NiRW wire and (b) V_1 (continuous lines) and V_3 (discontinuous lines) for all samples. The energy applied to the conductors was $Q = 49, 16, 13, 9$ mJ and $t_p = 40, 12, 11, 6$ ms for the samples NiRW, FeRW, FeT and Fe4SW, respectively. The heater current pulse starts at $t = 0$. For the Fe-sheathed conductors, the current was turned to zero at $t \sim 0.35$ s to prevent damaging the conductor.

around the heater that propagates along the conductor, as shown in figure 4(a). The shoulder observed on the $E(t)$ curves would mark the complete transition from the superconducting to the normal state of the zone measured by the voltage taps.

The measured voltages V_1 and V_3 after a quench for all samples at $T_0 = 20$ K and $I = 100$ A are plotted in figure 4(b), which clearly shows the differences among the conductors with regard to their normal-resistivity values, and to the superconductor–normal transition, this being the sharpest for the FeT tape and the widest for the NiRW wire. Sharper transitions are expected when increasing the resistance of the metal sheath, ρ_m, and the n-values of the superconductor I–V characteristic. In our case, samples with very similar measured $n(T)$, such as NiRW and Fe4SW, show different behaviour, which, therefore, would be mainly attributed to the different electrical and thermal properties of their metal sheaths. Note that an increase of ρ_m, also associated to a decrease of the thermal conductivity, would further increase the local temperature. Moreover, it is observed that despite the difference on the normal electrical resistance among the analysed conductors, the quench propagates with similar velocity for all the Fe-sheathed conductors, while v_p is significantly lower for the Ni-sheathed wires, as it will be analysed later in more detail.
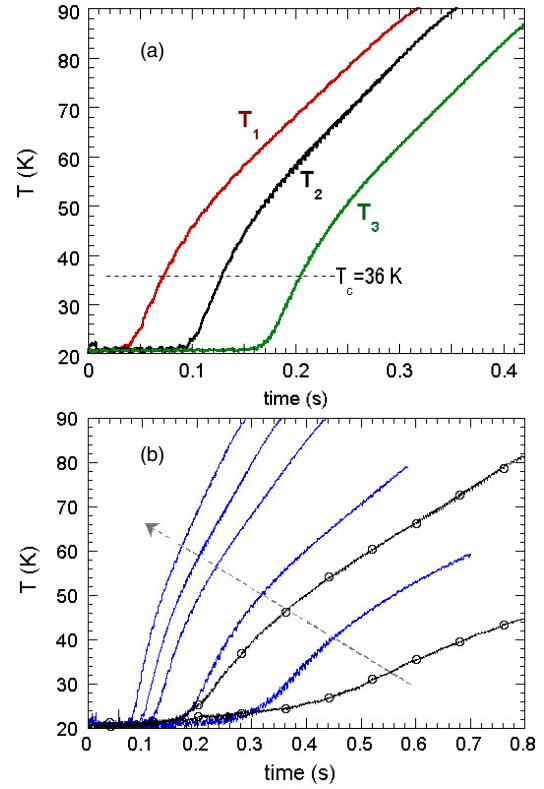
Figure 5. (a) Temperatures measured by the thermocouples after a quench for the Fe4SW square wire, for the same conditions as in figure 4. (b) Temperatures measured by the thermocouple T_2 at $T_0 = 20$ K after a quench for sample Fe4SW (lines without symbols and $I = 40, 60, 85, 100$ and 120 A) and NiRW (lines with symbols and $I = 60$ and 100 A). The arrow in (b) indicates increasing I.

The quench propagation can be also analysed from the time evolution of the temperatures measured by the thermocouples along the conductor (see figure 2). A typical measurement corresponding to the Fe4SW wire at the same conditions as in figure 4 is shown in figure 5(a). When a quench has been triggered the temperature of the conductor increases sharply, depending mainly on the current carried by the wire, I, as is seen in figure 5(b). It is observed that, as expected, the temperature increase during a quench is much sharper for the Fe-sheathed conductors because of their higher normal electrical resistance. On the other hand, for the same current but different initial temperatures, the measured $T(t)$ curves during a quench almost coincide when shifted by ΔT_0 (data not shown).

4.1. Quench propagation velocity (v_p)

The quench propagation velocities, v_p, have been obtained experimentally from the time delay to reach T_c of thermocouple T_3 with regard to T_1, and their position (see figures 2 and 5(a)). The current and temperature dependences of v_p estimated experimentally by this criterion are shown in figure 6 for all samples. Measured values range from 4 to 45 cm s^{-1} depending on the conductor and on the operation temperatures and currents. It must be noted that v_p has been also obtained from the delay to reach T_c of all thermocouples (T_1, T_2 and
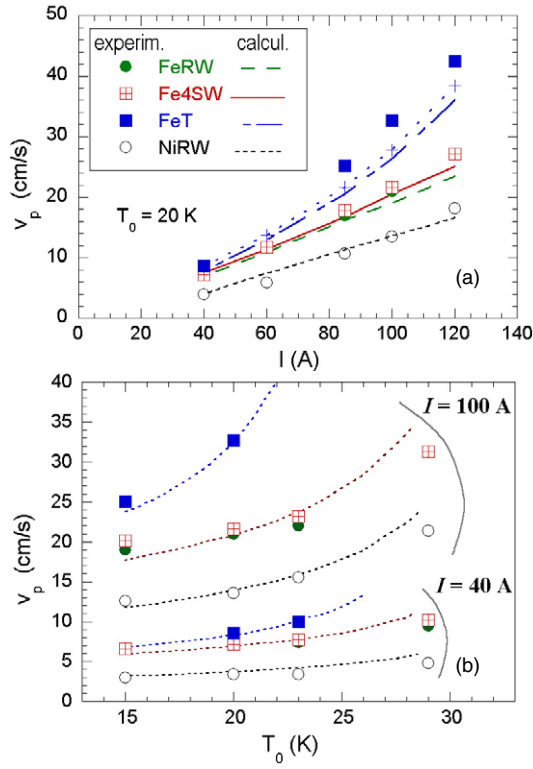
Figure 6. (a) Measured (symbols) and calculated (lines) quench propagation velocities for the different samples as a function of the current and $T_0 = 20$ K. The discontinuous line with symbols (- - + - -) corresponds to the function $v_p \propto I[T_g(I) - T_0]^{-1/2}$. (b) Measured v_p as a function of the temperature for $I = 40$ and 100 A. The same symbols as in (a) have been used. Discontinuous lines in (b) correspond to the function $v_p \propto [T_g(I) - T_0]^{-1/2}$. (Samples FeRW and Fe4SW show very similar behaviour and only the discontinuous line that corresponds to sample Fe4SW is shown for clarity reasons.)

T_3), and from the delay to reach the voltage value at the shoulder of the measured V_1, V_2 and $V_3(t)$ curves, which would mark the end of the superconductor-to-normal transition. The differences among these values are typically lower than 10–15%.

Figure 6(a) shows the v_p dependence on the transport current obtained experimentally (symbols) and numerically (lines) at $T_0 = 20$ K for all analysed conductors. As is observed, the experimental trends are well reproduced by the numerical estimations using 1D simulations. The $v_p(I)$ dependence is almost linear for most samples except for the FeT tape. Moreover, for a given transport current, v_p-values increase with the operation temperature, as is observed in figure 6(b).

As is known, v_p is determined by the temperature dependence of the thermal and electrical properties of the conductor, and the transport current density, as well as on the curve $T_g(I)$, which marks the temperature at which dissipation begins, and the current sharing temperature range (T_c–T_g). These dependences can be clearly observed in the approximate equation given by Wilson [8] for adiabatic conditions:

$$v_p = \frac{I}{A} \frac{1}{C} \left(\frac{\rho_n K}{T_s - T_0} \right)^{1/2} \qquad (4)$$

T_s being the temperature midway between T_g and T_c, and the other variables as in (1)–(3). Note that v_p will increase when T_0 approaches T_g because on the one hand the term $(T_s - T_0)^{-1}$ would increase, and also the averaged heat capacity between T_s and T_0, C, would decrease.

For the samples and conditions analysed here, we have observed that the dependence $v_p(I, T) \propto I[T_g(I) - T_0]^{-1/2}$, with different proportionality constants for each sample, almost reproduces the experimental values, as is seen in figures 6(a) and (b). Given that samples Fe4SW, FeRW and NiRW have similar critical currents (figure 1), the slower v_p obtained for the latter is most likely the result of its different thermal properties and normal sheath resistivity, consistent with figure 4(b). On the other hand, the deviation from linearity of the $v_p(I)$ curves would be determined by the current dependence of the term $[T_g(I) - T_0]^{-1/2}$, for the analysed current interval at a given operation temperature. At $T_0 = 20$ K, for sample FeT, which has the lowest critical current (figure 1) and exhibits the most pronounced nonlinearity in $v_p(I)$, $[T_g(I) - T_0]$ changes from ∼10 K at 40 A to 4 K at 120 A. For the other samples, this term varies by less than 15% for the same current range, and the corresponding $v_p(I)$ remains largely linear. The nonlinearity of $v_p(I)$ will become significant for all samples when the initial conditions (T_0, I) are in proximity to the critical current curve, i.e., $I/I_c(T_0) \sim 1$, hence ($T_g - T_0$) increases rapidly with reducing current I. Even if the $I_c(T)$-values of the FeT sample, shown in figure 1, were underestimated as discussed in section 2, these are the crucial values for quench development because once the temperature of the wire increases above this curve the superconductor will dissipate energy.

Moreover, the numerical simulations have shown that for the same T_g, v_p increases when the current sharing temperature range decreases. So, for example, a quench in a conductor with the same thermal properties as FeRW at $I = 100$ A and $T_0 = 20$ K would propagate at $v_p = 35$ cm s^{-1} if $T_g = 26$ K and $T_c = 35$ K, while $v_p = 55$ cm s^{-1} for the same conditions if $T_g = T_c = 26$ K.

4.2. Minimum propagating zones (MPZs)

After applying a heat pulse to the conductor, the temperature of the material may increase locally above T_g, causing the sharing of the current by the metal sheath and the superconducting core according to equation (2). When this zone is smaller than the so-called MPZ, it will eventually shrink, while if it is longer, it will grow indefinitely, originating a quench. In adiabatic conditions, as studied here, the size of the MPZ would depend mainly on the transport current density, the operation temperature and on the electrical and thermal conductivity of the composite [8]. In these experiments the heater length should be smaller than the MPZ in order to have a reasonable approximation to a point source [8, 24]. Nevertheless, for practical reasons the minimum heater length that we can prepare in our experimental set-up is 2–3 mm, which sets the limit of the smallest MPZ that can be ascertained by our set-up. For MPZs smaller than this limit, the MQE becomes overestimated.

Figure 7 shows the measured $V_1(t)$-values for different injected energies, Q_{ini}, at $T_0 = 20$ K and $I = 40$ A,
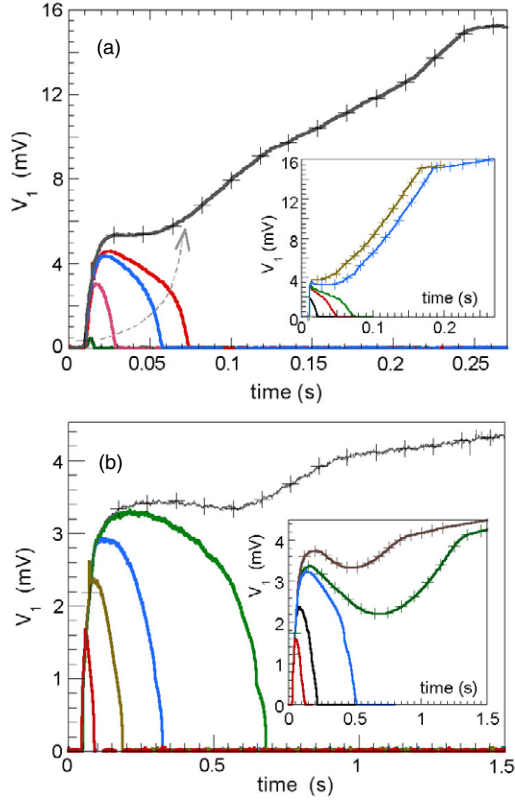
Figure 7. Measured and calculated (inset) $V_1(t)$ curves for the Fe4SW (a) and the NiRW (b) wires at 20 K and 40 A, for different Q_{ini}, for the cases of recovery (lines) and quench (lines with symbols). In (a) $Q_{ini} = 15.7, 17.1, 18.6, 20, 21.4$ mJ (exper.) and $Q_{ini} = 15.6, 17.0, 17.5, 18.2, 19.2$ mJ (calc., inset). In (b) $Q_{ini} = 68.5, 87.1, 99.6, 103.3, 104.6$ mJ (exper.) and $Q_{ini} = 58.5, 68.5, 77, 78.4, 82.2$ mJ (calc., inset). The arrow in (a) indicates increasing Q_{ini}.

for samples Fe4SW (figure 7(a)) and NiRW (figure 7(b)). In both cases, we observe that for certain values of Q_{ini}, part of the wire undergoes the transition to normal state, generating a voltage $V_1 > 0$, but eventually it recovers and V_1 decreases to zero. When we further increase Q_{ini}, a quench is developed (lines with symbols in the figure). Note that the experimental behaviour is in good qualitative agreement with the numerical simulations, shown in the insets of figure 7, although some differences on the Q_{ini}-values and on the exact shape of the $V_1(t)$ curves are observed. These differences ($\sim$10%) would be mainly attributed to the discrepancy in the thermal/electric properties between the model and the real sample. Moreover, the simplified 1D model used in the calculations does not account for 2D effects such as the conductor geometry and the resistive reactive layer between the sheath and the superconducting core observed in Ni- and Fe-sheathed MgB$_2$ conductors [4, 20].

Although both samples show the same qualitative behaviour, some important differences are observed. First of all, the maximum V_1 measured without triggering a quench is $V_{1,max} \sim 4.5$ mV for the Fe-sheathed sample, much lower than the voltage measured when the complete length scanned by V_1 is switched to normal state ($L_1 = 10$ mm, $V_1(T_c) = 15$ mV, see figure 7(a)). $V_1(T_c)$ corresponds to the value of V_1 at the
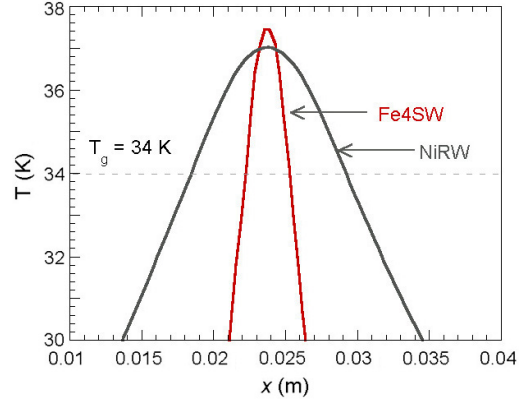

Figure 8. Calculated temperature profiles, $T(x)$, along the conductors Fe4SW and NiRW at 20 K and 40 A, at the time when V_1 becomes unstable. The contour conditions are $T = T_0$ at $x = 0$ and $x = 0.07$ m, as in the experiments (see figure 2). T_g at $I = 40$ A is 34 K in both samples.

shoulder observed on the $V_1(t)$ curve, as explained above. In contrast, for the Ni-sheathed sample, $V_{1,max} = 3.3$ mV is of the order of the voltage measured by V_1 when the conductor is in normal state ($L_1 = 11.5$ mm, $V_1(T_c) \sim 4.1$ mV, figure 7(b)). A rough estimation would give us MPZ values of 3 and 9 mm for Fe4SW and NiRW, respectively, at these conditions. On the other hand, note that the timescale of both graphs is different, so that for the NiRW sample, V_1 persists up to $t = 0.67$ s, when it drops to zero, while for Fe4SW, this happens at shorter times, $t = 0.075$ s.

The above estimation just gives an approximate value of the MPZ since the conductor dissipates at $T \geqslant T_g$, during current sharing, and therefore below T_c. One can also estimate the MPZ numerically by analysing the thermal profile, $T(x)$, along the conductor when V_1 just becomes irreversible (i.e. when the quench starts), as is observed in figure 7. Figure 8 shows the calculated $T(x)$ curves at that time for the same samples and conditions as in figure 7 ($T_0 = 20$ K and $I = 40$ A). It is seen that for the Fe4SW wire just a small part of the conductor (about 3 mm, which is of the order of the heater length) has been brought above the current sharing temperature ($T_g = 34$ K), while for NiRW, this is 11 mm. Therefore, that would give us an estimate of the MPZ of 3 and 11 mm for Fe4SW and NiRW, respectively, in agreement with the above experimental results. Using the same procedure we have estimated that the MPZ = 5 mm for FeRW at the same T_0 and I conditions.

The MPZ decreases when increasing I and T_0. For example, for the analysed Ni-sheathed wire, the MPZ decreases almost linearly with $(1/I)$, giving MPZ = 11, 7 and 5.5 mm for applied currents of 40, 60 and 85 A, respectively at $T_0 = 20$ K. On the other hand, for a given transport current the MPZ decreases very slowly when increasing T_0 except when approaching $T_g(I)$. This way, the estimated MPZ values for the same sample and at $I = 40$ A are approximately 12, 11, 9.5 and 7 mm at $T_0 = 15, 20, 23$ and 29 K, respectively.

When increasing the current above a certain limit, which depends on the sample and on T_0, a quench occurs whenever $V_1 > 0$, i.e. the case of measuring $V_1 > 0$ with subsequent recovery is never observed. This behaviour can be explained
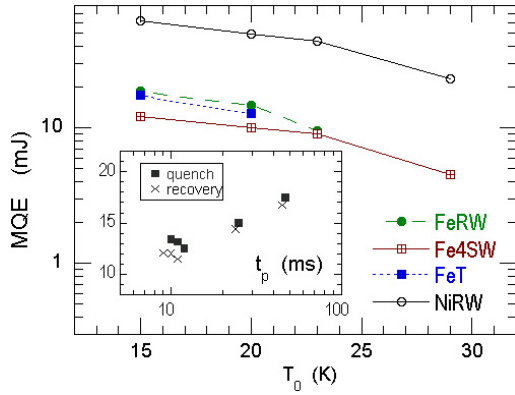
Figure 9. MQE values for the different samples at $I = 100$ A as a function of the operation temperature. The inset shows the dependence of the MQE (in mJ) on the duration of the pulse, t_p, for the FeT tape at $T_0 = 20$ K and $I = 100$ A.

if the actual MPZ is smaller than the heater length, L_h, so that the smallest normal zone we can create is always bigger than the MPZ. Therefore for these cases one just can conclude that MPZ $< L_h$. For example, at $T_0 = 20$ K this has been observed at $I > 40$, 60, 85 and 110 A for samples FeT, Fe4SW, FeRW and NiRW, respectively.

4.3. Minimum quench energy (MQE)

Minimum quench energies decrease when increasing the operation temperatures and currents. The experimental MQE values range typically from 5 to 35 mJ for the Fe-sheathed samples and from 20 to 80 mJ for the Ni-sheathed sample, differences that would be related to their MPZ values. Figure 9 shows the MQE at $I = 100$ A for all analysed samples. It is observed that the MQEs for these conductors are higher than in LTSs [9, 10], probably because of the higher operating temperatures of MgB$_2$, and considerably smaller than in HTSs [13]. Nevertheless, the obtained MQE may be overestimated because of the following effects. On the one hand, in our experiments the dissipated power in the heater, $V_h I_h$, was 1.3–1.5 W in all cases, and therefore the pulse duration for the NiRW measurements are longer than in the rest of the samples. Since the MQE increases with the pulse duration, t_p, as is seen in the inset of figure 9, the actual MQE may be slightly smaller in some cases. Moreover, we have observed that the experimental values can be reproduced by the numerical simulations if we take into account the mass and heat capacity of the heater itself ($C = 0.07$ J g^{-1} K^{-1} at $T = 30$ K). When this contribution is neglected, estimated MQE values are smaller than the experimental ones, by a factor of two, approximately. The other parameters, v_p and MPZ, should not be affected by this.

4.4. Influence of the sample length

For quench development and propagation studies the heater and the voltage taps and thermocouples should be placed at a sufficient distance from the contour-condition points ($x = 0$, $x = L$), so that the observed behaviour would be independent of the wire length. Clearly, this minimum distance increases

with the size of the MPZ. Since the numerical simulations can reproduce approximately the observed experimental behaviour related to the v_p and MPZ values, we have used these simulations to determine whether the conductor length used here is sufficient for quench propagation experiments, and therefore if the observed behaviour applies to longer samples for the analysed conductors at the different current and temperature conditions.

With this purpose, we have performed simulations for a much longer sample (70 cm, instead of 7 cm) with the heater placed in the middle ($x = 35$ cm), and the thermocouples and voltage taps also far away from the contour points (distance from $x = 0$ and $x = L$ greater than 25 cm). Note that in this case, the wire would be almost two orders of magnitude longer than the largest MPZ of the studied samples and conditions (1.1 cm). In this regard, we have seen that only for the NiRW sample, with higher electrical and thermal conductivity, and at low currents ($I < 60$ A), are the thermal profiles $T(x, t)$ after a quench affected by the imposed contour conditions on the 7 cm long sample. Nevertheless, the effect on the estimated parameters is small. For example, numerical simulations of a 7 and a 70 cm long NiRW wire at $I = 40$ A and $T_0 = 20$ K give an increase of v_p from 4.1 to 4.5 cm s^{-1} and a decrease of MPZ from 11 to 10 mm, respectively. Also the MQE value is affected, with a decrease of about 15% on the longest wire.

5. Conclusions

We have obtained experimentally and numerically the parameters characterizing quench development and propagation in Fe- and Ni-sheathed MgB$_2$ conductors, focusing on the estimation of MPZ, v_p and MQE values. The measurements were done at self-field and in vacuum for variable operation currents and temperatures. We have observed qualitative agreement between the experimental results and the numerical simulations obtained by solving the 1D heat flow equation and using the experimentally obtained $I_c(T)$, $n(T)$ and thermal properties of the conductors. The numerical calculations have been used to determine the influence and limitations of the finite-length conductors used in the experiments, as well as to analyse the effect of the relevant parameters on quench propagation. Further improvements of the model would require us to implement the 2D model in order to analyse the effect of the resistive reactive layer between the sheath and the superconducting core observed in Ni- and Fe-sheathed MgB$_2$ conductors [4, 20].

The quench propagates with velocities ranging from 4 to 45 cm s^{-1}, which increases mainly with I, although an influence from the temperature dependence of the thermal properties, the operation temperature and $I_c(T)$ has also been observed. MPZ values are generally lower than 1–1.5 cm and the MQE is of the order of 5–80 mJ. Both MPZ and MQE values are mainly limited by the thermal properties of the sheath material, so they are higher for the Ni-sheathed wire, which has higher thermal and electrical conductivity. Further improvement of the thermal stability of MgB$_2$, associated to an increase of the MPZ and MQE values, would be required, by introducing a high thermal-conductivity metal in the sheath/matrix, such as high RRR copper, and by avoiding the formation of the resistive layer between the MgB$_2$ filaments and the metal sheath. Moreover, it must be noted that for

magnet applications, MPZ and MQE would be higher than the values obtained here, because the heat also spreads sideways from turn to turn in the windings.

Acknowledgments

References

[1] Zhao Y, Feng Y, Cheng C H, Zhou L, Wu Y, Machi T, Fudamoto Y, Koshizuka N and Murakami M 2001 *Appl. Phys. Lett.* **79** 1145

[2] Suo H L, Beneduce C, Dhallé M, Musolino N, Genoud J E and Flűkiger R 2001 *Appl. Phys. Lett.* **79** 3116

[3] Cimberle M R, Novak P, Manfrinetti P and Palenzona A 2002 *Supercond. Sci. Technol.* **15** 43

[4] Kováč P, Hušek I and Melišek T 2002 *Supercond. Sci. Technol.* **15** 1340

[5] Fu B Q, Feng Y, Yang G, Liu C F, Zhou L, Cao L Z, Ruan K Q and Li X G 2003 *Physica* C **392–396** 1035

[6] Goldacker W, Schlachter S I, Obst B and Eisterer M 2004 *Supercond. Sci. Technol.* **17** S490

[7] Holúbek T, Kováč P and Melišek T 2005 *Supercond. Sci. Technol.* **18** 1218

[8] Wilson M N 1983 *Superconducting Magnets* (Oxford: Clarendon) p 76 and 206

[9] Ghosh A K and Sampson W B 1997 *IEEE Trans. Appl. Supercond.* **7** 954

[10] Wilson M N and Wolf R 1997 *IEEE Trans. Appl. Supercond.* **7** 950

[11] Kimura A, Kim S W, Kimura N, Makida Y, Shintomi T, Hirabayashi H, Mito T, Iwamoto A and Yamamoto J 1995 *IEEE Trans. Appl. Supercond.* **5** 385

[12] Tasaki K, Kuriyama T, Nomura S, Sumiyoshi Y, Hayashi H, Kimura H, Tsutsumi K, Iwakuma M and Funaki K 2003 *Physica* C **392–396** 1210

[13] Wang X R, Caruso A R, Breschi M, Zhang G M, Trociewitz U P, Weijers H W and Schwartz J 2005 *IEEE Trans. Appl. Supercond.* **15** 2586

[14] Grabovickic R, Lue J W, Gouge M J, Demko J A and Duckworth R C 2003 *IEEE Trans. Appl. Supercond.* **13** 1726

[15] Fu M, Zhengquan P, Zhengquan J, Kumakura H, Togano K, Ding L, Wang F, Zhang Y, Chen Z and Chen J 2004 *Supercond. Sci. Technol.* **17** 160

[16] van Weeren H, van den Eijnden N C, Rabbers J J, Ilyin Y, Dhallé M and den Ouden A 2003 *Inst. Phys. Conf. Ser. (EUCAS 2003)* vol 181 (Bristol: Institute of Physics Publishing) p 648

[17] Ishiyama A and Asai H 2001 *IEEE Trans. Appl. Supercond.* **11** 1832

[18] Vysotsky V S, Rakhmanov A L and Ilyin Yu 2004 *Physica* C **401** 57

[19] Kováč P, Hušek I, Melišek T, Dhallé M, Müller M and den Ouden A 2005 *Supercond. Sci. Technol.* **18** 615

[20] Martínez E, Millán A A and Navarro R 2003 *Inst. Phys. Conf. Ser. (EUCAS 2003)* vol 181 (Bristol: Institute of Physics Publishing) p 2502

[21] Flükiger R, Suo H L, Musolino N, Beneduce C, Toulemonde P and Lezza P 2003 *Physica* C **385** 286–305

[22] Lezza P, Gladyshevskii R, Suo H L and Flükiger R 2005 *Supercond. Sci. Technol.* **18** 753

[23] Young E A and Yang Y 2006 in preparation

[24] Scott C A 1982 *Cryogenics* **22** 577